

The nature of the activity in Hickson compact groups of galaxies.

Roger Coziol¹, André L. B. Ribeiro²

Reinaldo R. de Carvalho³

and

Hugo V. Capelato²

Received _____; accepted _____

¹Laboratório Nacional de Astrofísica - LNA/CNPq, Rua Estados Unidos, 154, Bairros das Nações - 37500-000 - Itajubá, MG, Brasil

²Divisão de Astrofísica - INPE/MCT, C.P. 515 - 12201-970 - S. José dos Campos, SP, Brasil

³Observatório Nacional, Rua Gal. José Cristino, 77 - 20921-400 - Rio de Janeiro, RJ, Brasil

ABSTRACT

We present the results of the spectral classification of the 82 brightest galaxies in a sample of 17 compact groups. We verify that the AGNs are preferentially located in the most early-type and luminous galaxies of the groups, as is usually observed in the field. But these AGNs also appear to be systematically concentrated towards the central parts of the groups. Our observations suggest a correlation between activity types, morphologies and densities of galaxies in the compact groups. This is consistent with a scenario in which galaxies of compact groups evolve by interacting with their environment and are currently in a quiet phase of their activity.

Subject headings: galaxies: Compact groups – galaxies: Seyfert – galaxies: LINERs – galaxies: interactions

1. Introduction

One of the important aspects of the study of the Hickson compact groups of galaxies (HCGs; Hickson 1982) resides in the attractive possibility of assessing the effects of strong interactions on the morphology and stellar content of galaxies (Hickson et al. 1992). The available data on the HCGs however seems to present many contradictions with a fast merging evolution scenario, suggesting that we still do not fully understand the nature of these systems. To shed new light on this problem a new spectroscopic survey of faint galaxies in the regions of Hickson compact groups was recently undertaken by de Carvalho et al. (1997; see also Ribeiro et al. 1997) to determine the kinematical structure of the groups. These studies show that HCGs exhibit a variety of dynamical configurations as opposed to the previous view that they are all isolated and high density structures.

Spectroscopic observations of galaxies around HCGs not only allow to establish how isolated these structures are from other structures but also yield valuable information on the nature of the activity of the individual groups. Previous studies on the activity of the galaxies in compact groups have led to contradictory conclusions. Recently, for example, Sulentic & Rabaça (1993) and Vignugopal (1995) contest the claim by Hickson et al. (1989a) that the far infrared emission is enhanced in compact groups. Radio observations (Menon, 1992,1995), optical spectroscopy and imaging (Rubin et al. 1991) all suggest that tidal interactions and mergers between compact group galaxies did happen in the past. However, many galaxies in the groups seem to be normal and it is not clear which phenomenon, either starburst or AGN, is the main source of activity observed in the groups. One extreme example of activities encountered in a compact group is HCG 16, which includes one Seyfert 2 galaxy, two luminous LINER galaxies and 3 starburst galaxies (Ribeiro et al 1996). But in a sample of 17 groups, HCG 16 is the only one of its kind, which suggests that in general the activity in the groups is not prominent.

In this contribution we present the results of our classification of the activity types of a sample of luminous galaxies from 17 HCGs. We show that a significant fraction of these galaxies display AGN activity. Moreover, 50% of the AGN population in the groups as studied here are “low-luminosity” AGNs (LLAGNs) – that is, faint AGNs, either Seyfert 2 or LINER, which are hidden behind the strong stellar continuum of their host galaxy. We also show that the AGN population always appears segregated towards the compact cores (which generally encompass most of Hickson’s original compact groups, Ribeiro et al. 1997) whereas starburst galaxies tend to be distributed in their external parts.

The organization of the paper is as follows. In Section 2 we define our sample of compact group galaxies and explain the criteria that we used to do our classification. We also present the characteristics of the LLAGNs in our sample and show the results of template subtraction, which is an essential part of the classification scheme. Section 2.1 presents the results of our classification of all the emission line galaxies following two diagnostic diagrams of line ratios. A brief discussion on the low-luminosity nature of the LLAGNs follows in Section 2.2. In Section 3, we discuss the spatial and morphological distribution of the active galaxies in the compact groups. We conclude, in Section 4, with a brief digression on the significance of our findings for the understanding of the nature of compact groups.

2. Spectral classification of the AGNs candidates

The spectra presented in this paper are part of a sample of 316 galaxies in the regions of 17 HCGs which were observed by de Carvalho et al. (1997). The spectra were taken at the 4m CTIO telescope using the ARGUS fiber-fed spectrograph. The details of the instrumental setup and data reduction are discussed by de Carvalho et al. (1997). In this sample, 82 galaxies (of which only 67 are kinematically assigned to the groups: see de

Carvalho et al. 1997) have spectra with sufficiently high S/N to allow a proper classification of the activity type. Of these galaxies, 28 (34%) present only absorption lines and 54 (66%) present both emission and absorption lines. In this article the non-emission line galaxies are considered non-active. A complete analysis of the absorption features in these galaxies will be published elsewhere (Coziol et al. in preparation). This article is dedicated to the classification of the emission-line galaxies.

Luminous emission-line galaxies are usually easy to identify and classify. These galaxies are either starburst or AGN galaxies. For many galaxies in our sample, however, the usual classification criteria cannot be applied directly, since they do not show any emission lines (i.e. within the limits of our observations) with the exception of the $[\text{N II}]\lambda 6584$ line. Figure 1 shows the spectra for these galaxies. The great similarity of the spectra suggests that either all these galaxies are of similar morphological type or they are dominated by the same stellar populations. Trace of ionized gas in early-type spirals and ellipticals was already observed before and it is generally suggested that a mild Seyfert or LINER, that is a low-luminosity AGN, could reside in the nuclei of all these galaxies (see Filippenko & Sargent 1985, Phillips et al. 1986; hereafter PJDSB). Given the similarity of the phenomenon observed here, we will provisionally call the subsample of the galaxies displayed in figure 1 the LLAGNs candidates. The basic characteristics of the LLAGN candidates are presented in Table 1. The numbers in columns 1 and 2 follow the numbering used in de Carvalho et al. (1997) and the letters in column 3 correspond to the galaxies in the Hickson (1982) list. Redshifts determined by de Carvalho et al. (1997) are listed in column 4. The B luminosities, as taken from Hickson et al. (1989), are listed in column 5. The absolute magnitudes, presented in column 6, were determined assuming $H_0 = 75 \text{ km s}^{-1} \text{ Mpc}^{-1}$. In column 7 we give also the morphologies of the galaxies, as reported by Mendes de Oliveira & Hickson (1994).

In the LLAGN candidates, the presence of an intermediate-age stellar population introduces strong Balmer absorption lines that interfere with the observation of faint ionized regions. The problem of detecting and measuring weak emission lines atop a strong stellar continuum has already been tackled by several groups of investigators in the past. Subtraction of a template galaxy spectrum that has no comparable emission has proved to be an effective technique. For our analysis we have taken advantage of having in hand a significant number of absorption–line galaxies, all observed under the same instrumental conditions, in order to build such a template. The spectral characteristics of the galaxies used as templates are remarkably similar to those of the LLAGN candidates. On average, the difference between the velocity dispersion of the absorption lines of our template galaxies and those of the LLAGN candidates is approximately 2 \AA , which is smaller than our resolution ($\sim 6 \text{ \AA}$). Figure 2 shows the red part of the spectra of the LLAGN candidates after template subtraction. Note the high $[\text{N II}]\lambda 6584/\text{H}\alpha$ ratios typical of AGNs.

The classification of the activity type of all the 54 emission-line galaxies in our sample was determined after subtraction of a galaxy template. The emission–lines were measured by fitting gaussian profiles. Our classification is based on the characteristic line ratios shown by galaxies of different activity classes (Baldwin et al. 1981; Veilleux & Osterbrock 1987). The emission–line galaxies in our sample were separated into 3 groups: starburst galaxies, AGNs and LLAGNs.

The first diagnostic diagram, presented in Figure 3, is the diagram of $[\text{N II}]\lambda 6584/\text{H}\alpha$ vs. $[\text{O III}]\lambda 5007/\text{H}\beta$ (Baldwin et al. 1981; Veilleux & Osterbrock 1987). The distinction between AGN and starburst galaxies is based on the empirical separation proposed by Veilleux & Osterbrock (1987). The separation between LINER and Seyfert 2 galaxies corresponds to $\log([\text{O III}]\lambda 5007/\text{H}\beta) \leq 0.4$, as proposed by Coziol (1996). The same criterium is used to distinguish between the low–excitation Starburst Nucleus Galaxies

(SBNGs) and the high-excitation HII galaxies. This diagnostic diagram confirms the AGN nature of all our LLAGN candidates. It also indicates that the majority of these galaxies are LINER galaxies.

To double check our classification we also examined the ratio $[\text{O I}]\lambda 6300/\text{H}\alpha$. As was shown by Baldwin et al. (1981), the presence and the strength of the $[\text{O I}]\lambda 6300$ are important factors in distinguishing between starburst galaxies and AGNs. This is because this line is produced only in regions of partial ionization which are much more extended in AGNs than in normal HII regions. For this reason the $[\text{O I}]$ line is rarely observed and is always weaker in starburst galaxies than in AGNs. In our sample, the $[\text{O I}]$ line is detected in 61% of the starburst galaxies, 88% of the LLAGNs and 60% of the AGNs. It is interesting to note that the detection rate of $[\text{O I}]$ in the starburst galaxies is much higher than usually observed in other samples of starburst nucleus galaxies (generally of the order of 40% or less; see Coziol et al. 1997).

In Figure 4, we present the diagnostic diagram of the ratio $[\text{O I}]\lambda 6300/\text{H}\alpha$ vs. $[\text{O III}]\lambda 5007/\text{H}\beta$. The vertical line is the $[\text{O I}]$ strength limit as proposed by Baldwin et al. (1981) to separate the starburst galaxies from the AGNs. This diagram confirms the nature of the LLAGNs as determined using the previous diagnostic diagram. Only one candidate (otherwise a seyfert galaxy) has an $[\text{O I}]$ line with strength comparable to those of starburst galaxies. Three other galaxies have values with error bars that cross the boundary between the two activity classes. The fact that many starburst galaxies in our sample have an unusually strong $[\text{O I}]$ line is consistent with previous observations suggesting that a small fraction of these galaxies show the simultaneous characteristics of an AGN and an HII region (Véron et al. 1996). Our result suggests that very few AGNs present the same ambiguity.

In Table 2, we list the results of our classification. The name of the objects are the

same as in Table 1. Columns 2, 3 and 4 give the ratios $[\text{O III}]\lambda 5007/\text{H}\beta$, $[\text{N II}]\lambda 6584/\text{H}\alpha$ and $[\text{O I}]\lambda 6300/\text{H}\beta$ respectively. The uncertainties in these ratios were determined using Poisson statistics. In column 5, the different types of activity are described as: starburst galaxies (SBNGs or HII), AGNs (Seyfert 2: Sy2 or LINER: LNR) and LLAGNs (dSy2 or dLNR). Column 7 give the FWHM of the $\text{H}\alpha$ line. It may be interesting to note that no Seyfert 1 galaxies was found in the groups.

2.1. The low-luminosity nature of the hidden AGNs

Rubin et al. (1991) already noted that all the elliptical and the S0 galaxies in the HCGs have ionized gas. They also remarked that this phenomenon is commonly observed in samples of early-type galaxies (PJDSB). But because the emission is hidden in the strong stellar continuum the nature of the activity in these galaxies was not clearly established. The subtraction of a template galaxy allow us to construct two different diagnostic diagrams which confirm the AGN nature of these objects. We will now verify that the AGNs in these galaxies also have a low luminosity. This will be done by comparing our candidates with the low-luminosity AGNs discovered by PJDSB.

Because we do not have the calibrated spectra of our candidates we cannot compare their fluxes directly with those of luminous AGNs. To test our assumption we use instead the EW of the $[\text{N II}]\lambda 6584$ line, which, by definition, is proportional to the ratio of the flux in the line divided by the stellar continuum near the line. In Figure 5 we compare the EW of the $[\text{N II}]\lambda 6584$ line as a function of the ratio $[\text{N II}]\lambda 6584/\text{H}\alpha$ for all the galaxies in our sample with those of the low-luminosity AGNs observed by PJDSB. A very clear pattern is seen: the LLAGNs have higher $[\text{N II}]\lambda 6584/\text{H}\alpha$ ratios and lower $\text{EW}([\text{N II}]\lambda 6584)$ than the luminous AGNs and the starburst galaxies. Most important, the values observed for the LLAGNs are identical to those of the low-luminosity AGNs as studied by PJDSB. It

is important to realize that in this diagram there is only one way to obtain the lowest EW value possible: the flux in the line must be low and the stellar continuum must be high. In early-type galaxies, as in the galaxies of the sample of PJDSB and also in our candidates (cf. figure 7), the stellar continuum is already near maximum, which means therefore that the line flux in the galaxies of these two samples must be similar. PJDSB determined that the characteristic $H\alpha$ luminosity of the low-luminosity AGN in their sample is of the order of 10^{39} ergs s^{-1} or lower. Then, by comparison, the luminosity of the AGNs in our candidates must be of the same order, which therefore confirms the low-luminosity nature of the AGNs in our objects.

3. Discussion

In Table 3 we present the fraction of each type of activity observed in our sample of 82 galaxies. The LLAGNs form more than 50% of the total AGN population found in the whole sample. From the 82 galaxies studied here, only 67 galaxies are real group members (de Carvalho et al. 1997). In Table 3 it can be seen that when only group members are considered, the fraction of starburst galaxies drops and the fraction for the other types slightly increases.

Going one step further, we can distinguish between the galaxies that reside in the “core” and the “halo” of the groups. As discussed by Ribeiro et al. (1997) most of HCG’s are embedded in larger structures forming extended haloes around more dense and dinamically distinct cores. As shown by Ribeiro et al. these cores may be usefully defined as the circular region around the group baricenter having mean surface brightness $\mu_B = 27$ mag arcsec $^{-2}$, which is almost the same limit used by Hickson (1982) as part of his criteria for constructing his catalogue of compact groups. Table 4 shows how the 67 galaxies in the groups distribute between the core (53 galaxies) and the halo (14 galaxies). It is

important to note that nearly all the AGNs, that is the LLAGNs as well as the luminous AGNs, reside in the core of the groups.

The fraction of each activity type encountered in the core regions is reported in Table 3. It can be seen that the fraction of starburst galaxies decreases significantly in the core of the groups, where AGNs (47.2%) and non-emission line galaxies (37.7%) dominate. Because the star formation rate in all of these galaxies is relatively low, we further conclude that the star formation rate in the groups is generally at a low level.

Our sample is obviously biased towards galaxies which have high S/N ratios, therefore favoring the most luminous galaxies in the groups. To verify how this bias affects our conclusions on the spatial segregation of the different activity types in the groups, we compare in Figure 6 the absolute magnitude of all the galaxies in our sample. In this figure we can see that the luminosity distributions for the LLAGNs and the luminous AGNs are clearly biased towards higher values. However Figure 6 also shows that both the non emission-line galaxies and the starburst galaxies show a comparable distribution of luminosities. Since these two types of galaxies have different spatial locations in the groups, we may conclude that the segregation of activity types in the groups is not due to a luminosity bias but corresponds to a real physical effect. The fact that AGNs reside in the most luminous galaxies of the groups is consistent with studies of AGNs in the field which show that the probability of finding an AGN increases with the luminosity of the host galaxy (PJDSB; Veilleux et al. 1995).

In Figure 7 we present the distribution of morphological types of all the galaxies in our sample. The LLAGNs reside either in elliptical or early-type spirals whereas the luminous AGNs seem to reside mostly in early-type spirals. Figure 7 also shows that all the non-emission galaxies are early-type galaxies (E, S0 or Sa). Consequently, the LLAGNs represent 36% (41% in the core) of the early-type population in the groups. This result is

consistent with the fraction of LLAGNs discovered by PJDSB in their sample of luminous E and S0 galaxies.

4. Conclusion

We have shown that a significant fraction of the brightest galaxies of compact groups display some sort of activity, either starburst or AGN. Moreover, we find that about half of the AGN population is made of LLAGNs, implying that AGNs are the most frequent activity types encountered in the groups.

We have further found that the AGNs – both low-luminosity and normal – reside in the most luminous galaxies of the groups and the most early-type ones. These two characteristics are not unique to compact groups but are consistent with the fact that the probability of finding an AGN increases with the luminosity of the galaxies and that low-luminosity AGNs are very common in early-type galaxies. However, we have also found that the AGNs tend to concentrate in the cores of the groups. This may be viewed as a consequence of the luminosity and/or a morphological segregation already found in the groups (Ribeiro et al. 1997). In other words, we have discovered a high fraction of AGNs in the cores of the groups because the most luminous and early-type galaxies are more concentrated in the groups and because the probability of finding an AGN is higher in luminous and early-type galaxies.

That the group produces some physical effects is even more obvious when we consider the starburst galaxies: the fraction of starburst galaxies drops drastically when we go from the halo to the core of the groups. It would be interesting to see if this behavior for the starburst galaxies is due to a morphological bias. In Figure 7 we can see that the starburst galaxies of our sample prefer late-type spirals. Although suggestive, this result should be

viewed with caution given the scarcity of the data for these galaxies (less than 20% of the morphologies determined in our sample).

As it is, our discovery suggests that we do have, at least for the core, a sort of density–morphology–activity relation. This relation may be reminiscent of the density–morphology relation observed in denser agglomerations of galaxies. For the HCGs, this relation would suggest that the galaxies in the groups have a common history and that their evolution was influenced by their environment.

As a working hypothesis we propose the following scenario for galaxy evolution in the HCGs. Massive galaxies form by subsequent mergers of smaller mass systems made of gas and stars. Obviously, denser environments will accelerate this process and the more massive galaxies will form first in the richest regions. The frequency and intensity of mergers determine the morphologies, the most massive galaxies evolving towards the most early–type morphologies. This would explain why in HCGs the most luminous galaxies are also the most concentrated and the most early–type.

This formation scenario can incorporate a sequence where the activity level changes with time. The first phase is characterized by a starburst and a Seyfert. Each merger triggers a starburst. When the mass of the galaxy is sufficiently high or when a large amount of gas is available, the gas falls into the center of the galaxy and form or nourish an AGN. As the starburst fades, depending on the reservoir of gas available and on the rate of accretion, it remains either a Seyfert or a LINER. Finally, when the matter available to feed the AGN decreases, it remains a LLAGN or a normal galaxy. This scenario would explain, for instance, the difference observed in the groups between the morphologies of the LLAGNs and the luminous AGNs. It would also explain why the core of the groups are dominated by a high fraction of LLAGNs and non–active early–type galaxies, since denser environments accelerate the process. The galaxies in the cores of the groups are more evolved than in the

outer regions. This would explain why starburst galaxies are observed in higher number in the halo than in the core. This scenario may also explain why we do not find any Seyfert 1 galaxy in the core, as they would be visible only at the beginning of the process.

Following this scenario, most of the activity in HCGs would have taken place sometime in the recent past, and the groups are now observed at a quiet phase of their activity.

We thank Natalie Stout for his careful reading of the manuscript. R. Coziol acknowledges the financial support of FAPESP under contract 94/3005-0 (while working at the Instituto Nacional de Pesquisas Espaciais/INPE) and of CNPq, under contracts 360715/96-6 (NV). For his part, A.L.B. Ribeiro acknowledges the support of the Brazilian CAPES.

Table 1. Characteristics of the low-luminosity AGNs

HCG #	Hickson id.	V_o km s^{-1}	B	M_B	Hubble Type
22–1	a	2681	12.6	-20.2	E2
22–5	d	9268	15.2	-20.3	E3
22–6	e	9611	15.2	-20.3	E5
23–3	a	4869	15.2	-18.8	Sab
23–5	c	5373	16.1	-18.1	S0
40–1	a	6634	14.3	-20.4	E3
42–1	a	3712	12.6	-20.8	E3
62–1	a	4259	13.3	-20.5	E3
64–1	...	6264	13.8	-20.8	...
67–11	...	6614	16.5	-18.2	...
86–1	a	6013	14.2	-20.3	E2
86–3	b	5863	14.8	-19.7	E2
87–1	a	8436	14.8	-20.4	Sbc
87–3	b	8738	15.4	-19.9	S0
88–1	a	6007	13.7	-20.8	Sb
88–2	b	6124	13.8	-20.8	SBb

Table 2. Spectral characteristics of HCG’s galaxies

HCG #	$\frac{[\text{OIII}]\lambda 50007}{\text{H}\beta}$	$\frac{[\text{NII}]\lambda 6548}{\text{H}\alpha}$	$\frac{[\text{OI}]\lambda 6300}{\text{H}\alpha}$	Activity Type	FWHM (km s ⁻¹)
04 01	-0.26	-0.31	-1.93	SBNG	535
04 03	-0.37	-0.32	-1.61	SBNG	367
04 11	0.77	-1.26	-1.96	HII	327
16 01	0.31 ± 0.02	0.09	-0.80 ± 0.04	LNR	498
16 02	0.58 ± 0.01	0.05	-0.40 ± 0.01	Sy2	816
16 03	0.12 ± 0.01	-0.35	-1.56 ± 0.18	SBNG	499
16 04	-0.35	-0.38	-1.91 ± 0.13	SBNG	489
16 05	0.35 ± 0.01	-0.22	-1.14 ± 0.04	LNR	533
16 06	0.61 ± 0.03	-0.8 ± 0.1	-1.07 ± 0.31	HII	383
19 05	-0.12	-0.495	...	SBNG	424
22 01	0.50 ± 0.03	0.03 ± 0.02	-0.9 ± 0.3	dSy2	953
22 05	0.50 ± 0.08	0.42 ± 0.02	-0.7 ± 0.4	dSy2	437
22 06	0.64 ± 0.08	0.23 ± 0.02	-0.7 ± 0.2	dSy2	518
22 07	-0.5 ± 0.1	-0.34 ± 0.02	...	SBNG	<360
22 08	...	-0.11 ± 0.01	...	LNR?	533
23 02	0.79	0.74	-0.11	Sy2	716
23 03	0.30	0.21	-0.49	dLNR	542
23 04	-0.25	-0.39	-1.78	SBNG	480
23 05	0.47	-0.09	-2.0 ± 0.1	dSy2	796
23 06	-0.21	-0.50	...	SBNG	356
40 01	0.0 ± 0.1	-0.06 ± 0.03	...	dLNR	560
40 04	0.1 ± 0.2	-0.19 ± 0.03	-0.9 ± 0.3	LNR	730
40 05	0.43 ± 0.05	-0.22 ± 0.02	...	Sy2	776
42 01	...	0.25 ± 0.01	-1.0 ± 0.5	dLNR	765
48 19	-0.29 ± 0.03	-0.54 ± 0.01	-1.4 ± 0.3	SBNG	392
48 25	0.36 ± 0.01	-0.96 ± 0.07	...	SBNG	366
62 01	0.00 ± 0.05	-0.22 ± 0.01	-1.1 ± 0.2	dLNR	795
63 04	0.11 ± 0.04	-0.18 ± 0.01	...	LNR	588

Table 2—Continued

HCG #	$\frac{[\text{OIII}]\lambda 50007}{\text{H}\beta}$	$\frac{[\text{NII}]\lambda 6548}{\text{H}\alpha}$	$\frac{[\text{OI}]\lambda 6300}{\text{H}\alpha}$	Activity Type	FWHM (km s ⁻¹)
63 06	-0.49 ± 0.06	-0.36 ± 0.01	...	SBNG	512
64 01	0.07 ± 0.05	0.42 ± 0.03	-0.8 ± 0.7	dLNR	701
64 22	-0.23 ± 0.08	-0.48 ± 0.02	-1.1 ± 0.2	SBNG	368
67 02	-0.15 ± 0.07	-0.47 ± 0.03	...	SBNG	658
67 06	-0.16 ± 0.04	-0.43 ± 0.03	...	SBNG	354
67 11	0.07 ± 0.14	0.71 ± 0.09	0.3 ± 0.2	dLNR	677
86 01	-0.40 ± 0.19	-0.21 ± 0.06	-0.6 ± 0.2	dLNR	402
86 03	0.95 ± 0.02	-0.08 ± 0.01	-1.1 ± 0.3	dSy2	947
86 04	0.17 ± 0.03	-0.15 ± 0.01	-0.83 ± 0.09	LNR	977
86 07	1.16 ± 0.01	0.09 ± 0.01	-0.37 ± 0.03	Sy2	728
86 08	-0.35 ± 0.04	-0.47 ± 0.01	-1.5 ± 0.2	SBNG	352
86 09	-0.10 ± 0.04	-0.66 ± 0.03	...	SBNG	763
87 01	0.08	-0.08	-0.500 ± 0.001	dLNR	601
87 02	-0.34	-0.42	-1.75 ± 0.01	SBNG	522
87 03	-0.35	0.11	...	dLNR	508
87 04	-0.38	-0.36	-0.76	SBNG	<360
87 05	0.31	-0.60	-1.14	SBNG	358
87 07	-0.08	-0.42	-1.65	SBNG	499
88 01	0.48	-0.05	-1.00	dSy2	704
88 02	0.18	0.28	-1.11	dLNR	517
88 07	0.10	-0.49	...	SBNG	231
90 01	0.97 ± 0.02	0.08 ± 0.01	-1.3 ± 0.8	Sy2	470
90 04	0.02 ± 0.07	-0.20 ± 0.01	-1.1 ± 0.2	LNR	441
90 09	0.21 ± 0.01	-0.61 ± 0.03	-1.4 ± 0.5	SBNG	359
97 05	0.23 ± 0.06	-0.28 ± 0.04	...	LNR	397
97 06	0.40 ± 0.04	-0.26 ± 0.03	...	Sy2	394

Table 3. Fraction of activity types

	all	in group	in core
No of Galaxies	82	67	53
No emission	34%	37.3%	37.8%
LLAGNs	20%	20.9%	24.5%
AGNs	18%	19.5%	22.6%
Starbursts	28%	22.3%	15.1%

Table 4. Classification of activity type

HCG	core				halo			
	(1)	(2)	(3)	(4)	(1)	(2)	(3)	(4)
04	1a
16	1a, 2b, 5d	...	3, 4c	6	...
19	1a
22	...	1a	...	3, 4b
23	...	3a, 5c	4d
40	4d,5e	1a	...	2b
42	...	1a	...	2b, 4c
48	1a	25	...
62	...	1a	...	2b, 3c, 4	8
63	4a	6	...
64	...	1	22	...
67	2b	1a, 3	...	11	6	...
86	4c	1a, 3b	...	6d	7	...	8, 9	2,10
87	4c	1a, 3b	2, 5
88	...	1a, 2b	7
90	1a, 4d	...	9	2b, 3c, 6
97	5, 6b	2, 4c, 3d	10, 11

Activity types: (1) = AGN; (2) = LLAGN; (3) = HII-SBNG; (4) = no emission.

REFERENCES

- Allam, S., Assendorp, R., Longo, G., Braun, M., Richter, G. 1996, *A&A*, 117, 39
- Baldwin, J. A., Phillips, M. M., Terlevich, R. 1981, *PASP*, 93, 5
- Coziol, R. 1996, *A&A*, 309, 345
- Coziol, R., Contini, T., Davoust, E., Considère, S. 1997, *ApJ*, 481, 67
- de Carvalho, R. R., Ribeiro, A. L. B., Capelato, H. V., Zepf, S. E. 1997, *ApJS*, 110, 1
- Ebeling, H., Voges, W., Boehringer, H. 1994, *ApJ*, 436, 44
- Filippenko, A. V., Sargent, W. L. W. 1985, *ApJS*, 57, 503
- Hickson, P. 1982, *ApJ*, 255, 382
- Hickson, P., Menon, T. K., Palumbo, G. G. C., Persic, M., 1989a, *ApJ*, 341, 679
- Hickson, P., Kindl, E., Auman, J. R. 1989b, *ApJ*, 341, 687
- Hickson, P., Mendes de Oliveira, C.M., Huchra, J.P., and Palumbo, G.G.C. 1992, *ApJ*, 399, 353
- Mendes de Oliveira, C., Hickson, P. 1994, *ApJ*, 427, 684
- Menon, K. 1992, *MNRAS*, 255, 41
- Menon, K. 1995, *MNRAS*, 274, 845
- Phillips, M. M., Jenkins, C. R., Dopita, M. A., Sadler, E. M., Binette, L. 1986, *AJ*, 91, 1062
- Ponman, T. J., Bournier, P. D. J., Ebeling, H., Boehringer, H. 1996, *MNRAS*, 283, 690
- Ribeiro, A. L. B., de Carvalho, R. R., Coziol, R., Capelato, H. V. & Zepf, S. E. 1996, *ApJ*, 463, 5
- Ribeiro, A. L. B., de Carvalho, R. R., Capelato, H. V., Zepf, S. E. 1997, *ApJ*, submitted
- Rubin, V. C., Ford, W. K. Jr., Hunter, D. A. 1991, *ApJS*, 76, 153

- Véron, P., Gonçalves, A. C., Véron–Cetty, M.-P. 1997, A&A, 319, 52
- Vegnugopal, V. R. 1995, MNRAS, 277, 455
- Veilleux, S., Osterbrock, D. E. 1987, ApJS, 63, 295
- Veilleux, S., Kim, D. -C., Sanders, D. B., Mazzarella, J. M., Soifer, B. T. 1995, ApJS, 98, 171

Fig. 1.— Optical spectra of the LLAGN candidates. The spectra are in the rest frame of the object. The flux scale was normalized to one and the spectra are shifted for presentation. Note the similarity of all the spectra. Nuclear activity is suggested by the presence of the Nitrogen emission line ($[\text{NII}]\lambda 6584$).

Fig. 2.— The spectra of the LLAGN candidates after subtraction of a template galaxy. The galaxies are shown in the same order as in Fig. 1. The ratios $[\text{NII}]\lambda 6584/\text{H}\alpha$ are high and $[\text{OI}]\lambda 6300$ is detected in almost all the galaxies.

Fig. 3.— Diagnostic diagram of emission–line ratio and classification of the different activity of our sample of emission–line galaxies. The dot-dashed line at $\log([\text{OIII}]/\text{H}\beta) = 0.4$ establishes a distinction between Seyfert 2 and LINERs (Coziol 1996). The solid line indicates the empirical separation between starburst galaxies and AGNs as determined by Veilleux and Osterbrock (1987).

Fig. 4.— Second diagnostic diagram of emission–line ratios. The vertical dashed line at $\log([\text{OI}]/\text{H}\alpha) = 1.3$ establishes a distinction between Starbursts and AGNs (Baldwin et al. 1981).

Fig. 5.— Equivalent widths (EW) of the $[\text{NII}]\lambda 6584$ line vs. its strength in comparison to $\text{H}\alpha$. The LLAGN possess a high ratio of $[\text{NII}]\lambda 6584/\text{H}\alpha$ and a low EW. The values for the LLAGN candidates in our sample are the same as those of the LLAGN studied by Phillips et al. (1986).

Fig. 6.— Distribution of the luminosities of the galaxies with different activity types in our sample. The AGNs are located in the most luminous galaxies of the groups, but the starbursts and the non emission galaxies show comparable luminosities. The low fraction of starburst observed in the core cannot be explain by a luminosity bias.

Fig. 7.— Distribution of the morphologies of the galaxies with different activity type in our sample. The LLAGNs and the non emission line galaxies are located in the most early-type galaxies of the groups. The luminous AGNs are mostly early-type spirals.

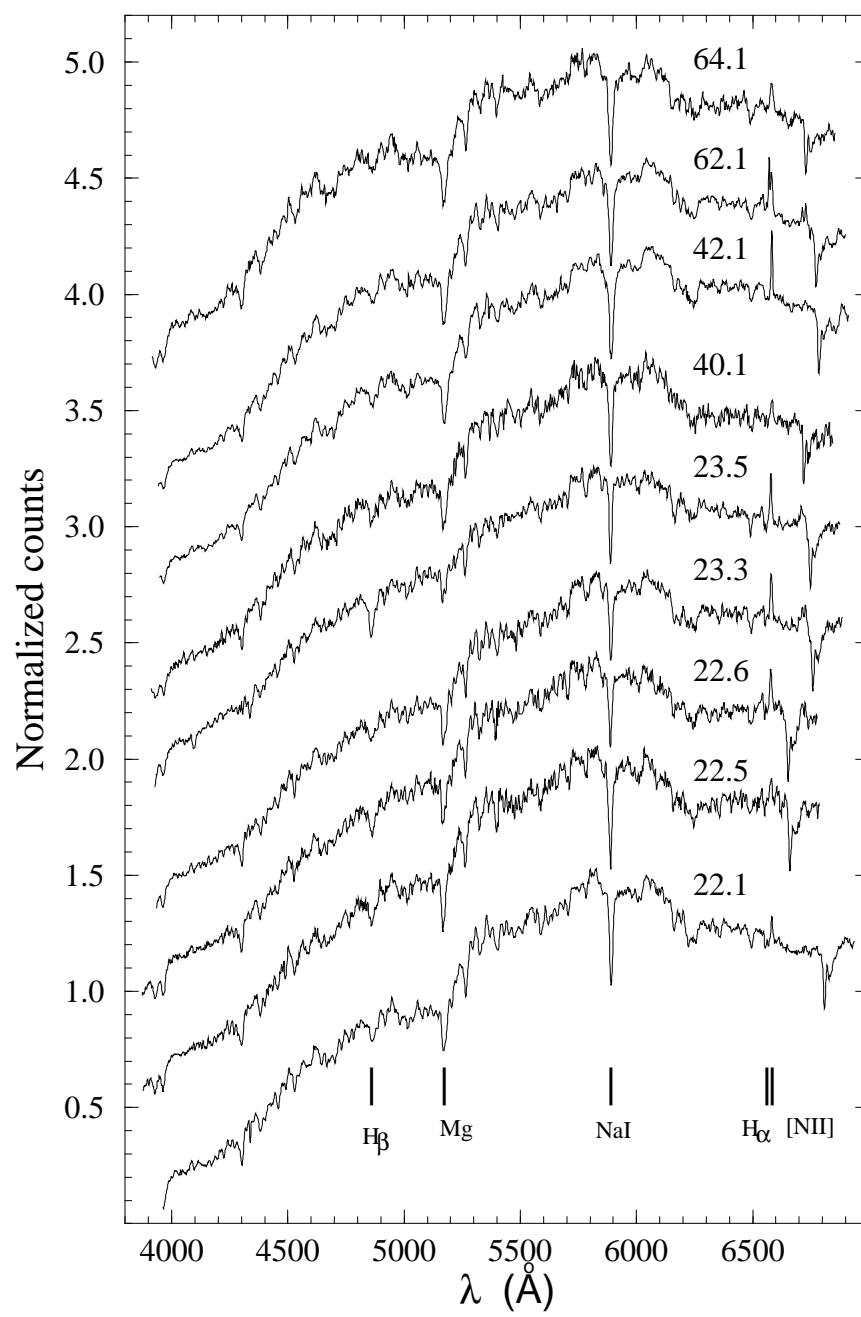


Fig. 1

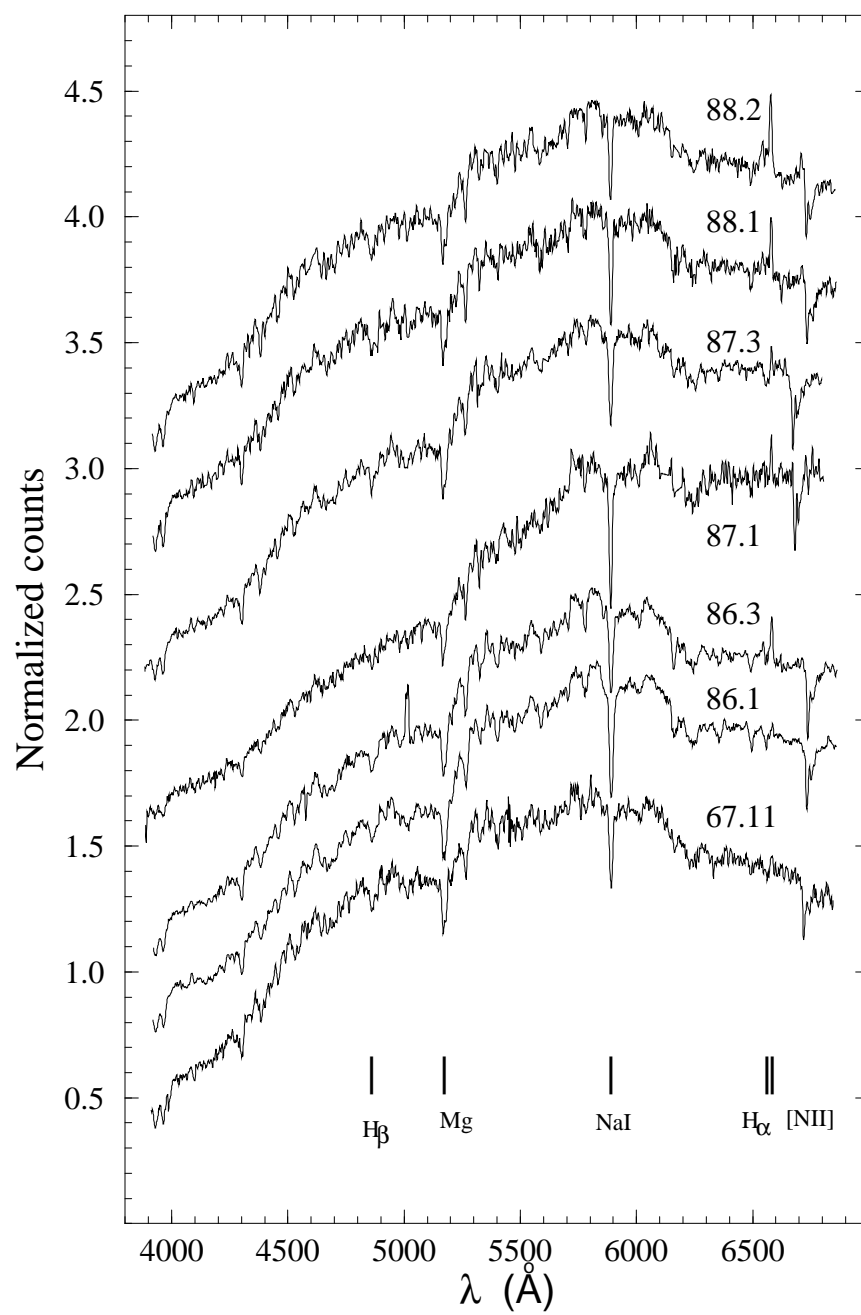


Fig. 1 (Continue)

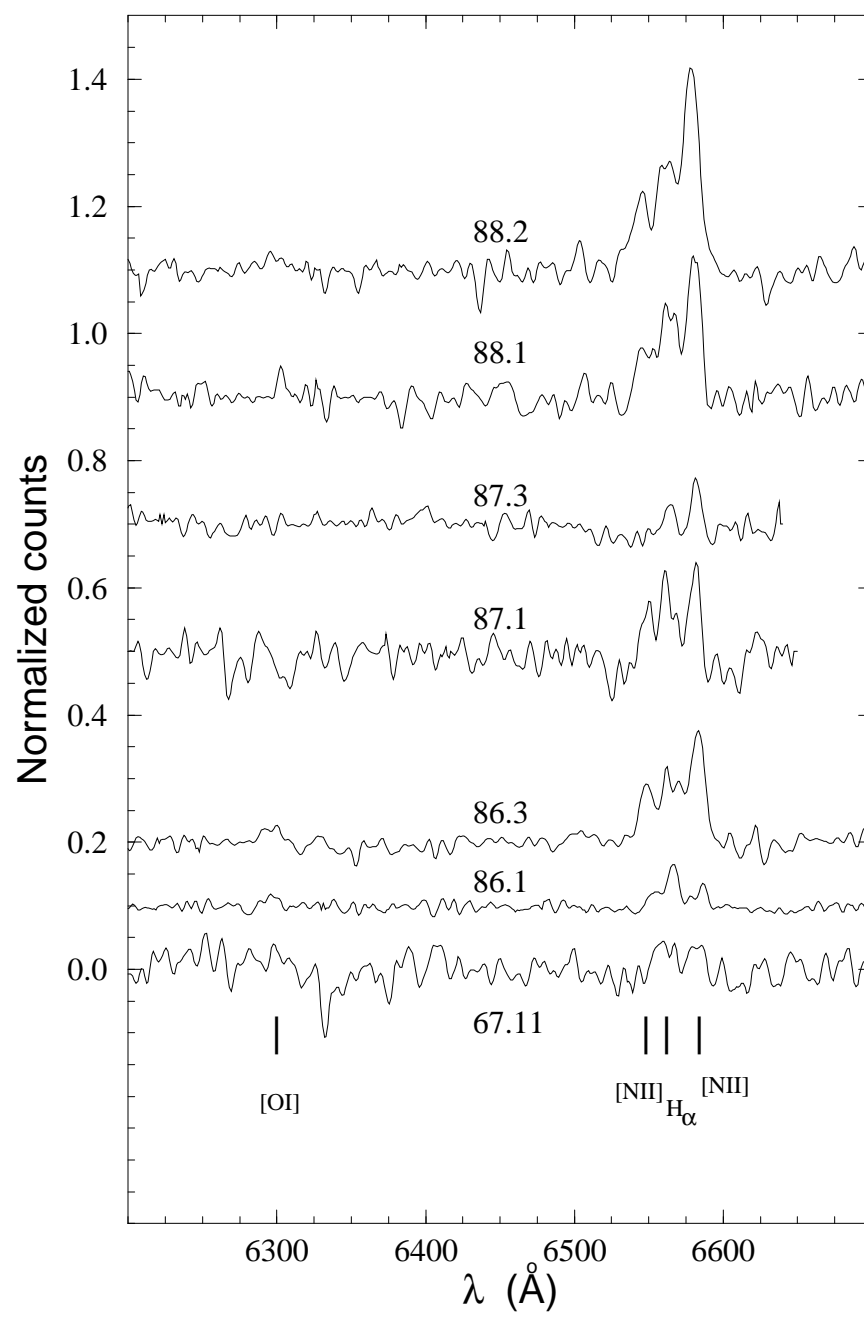


Fig. 2 (Continue)

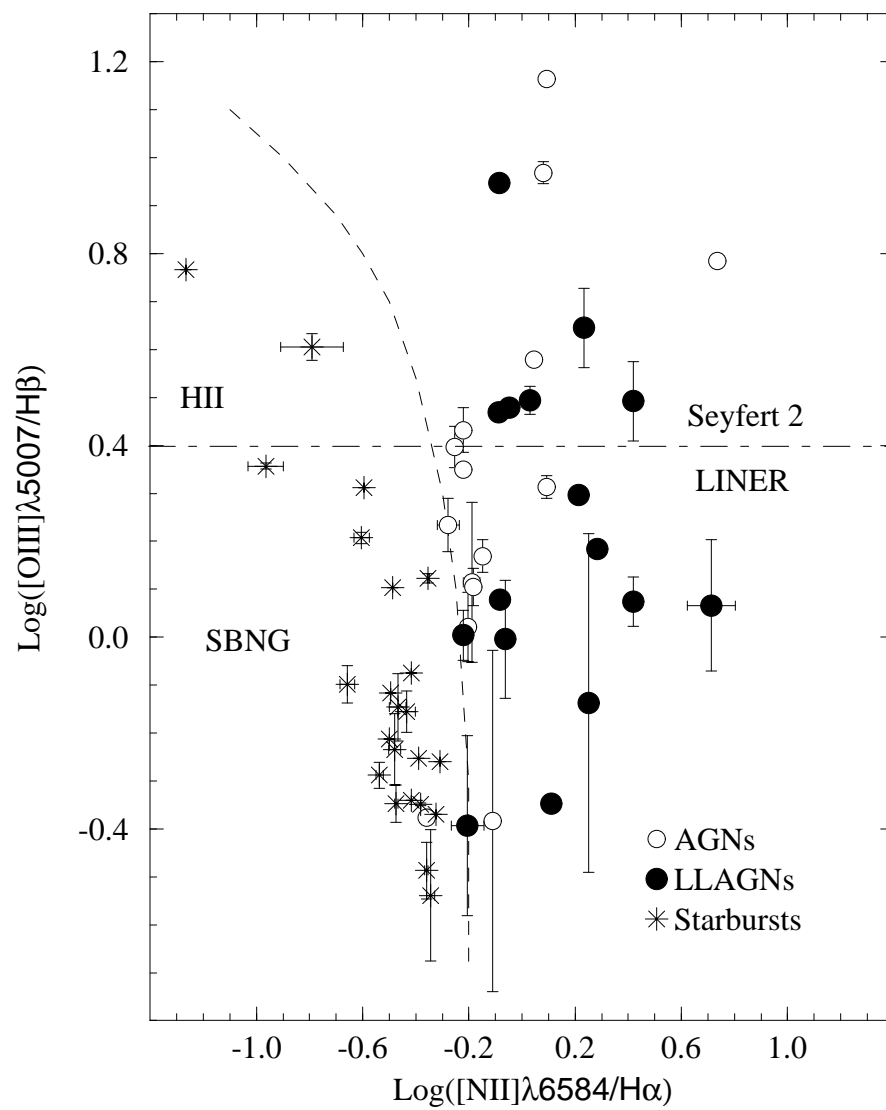


Fig. 3

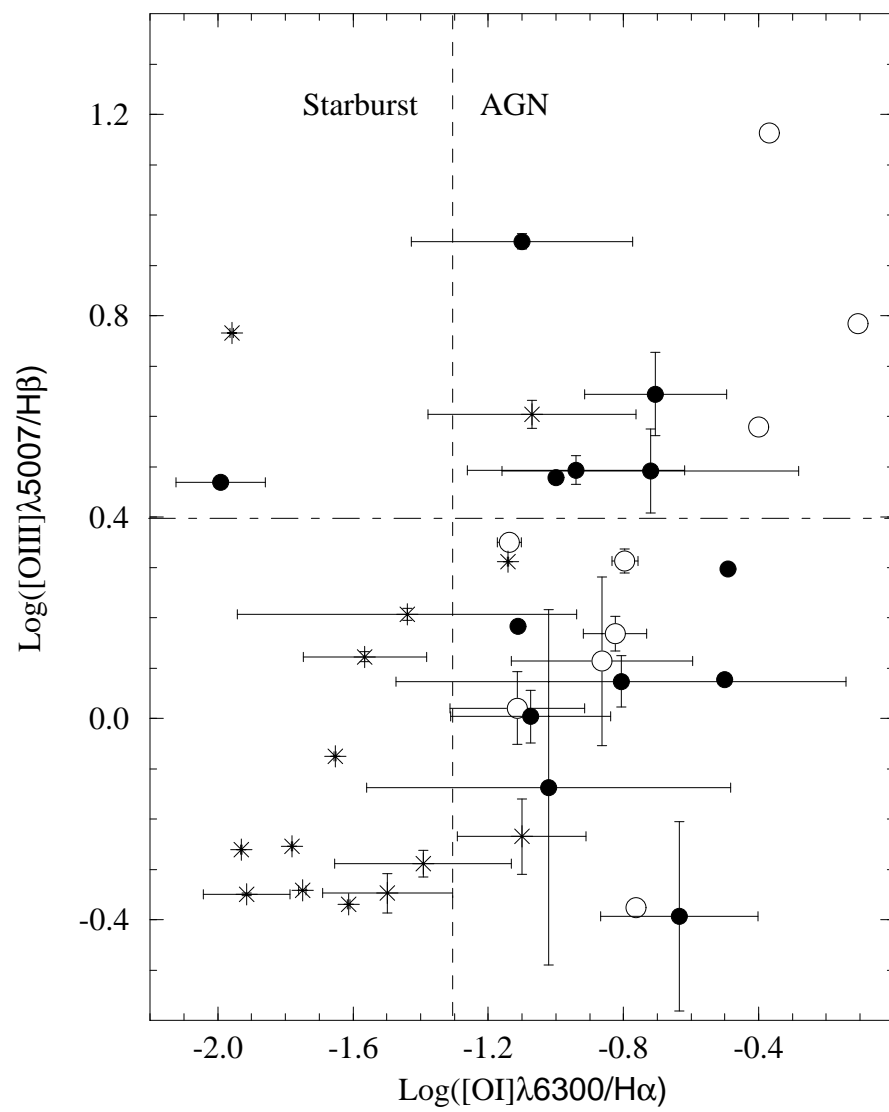


Fig. 4

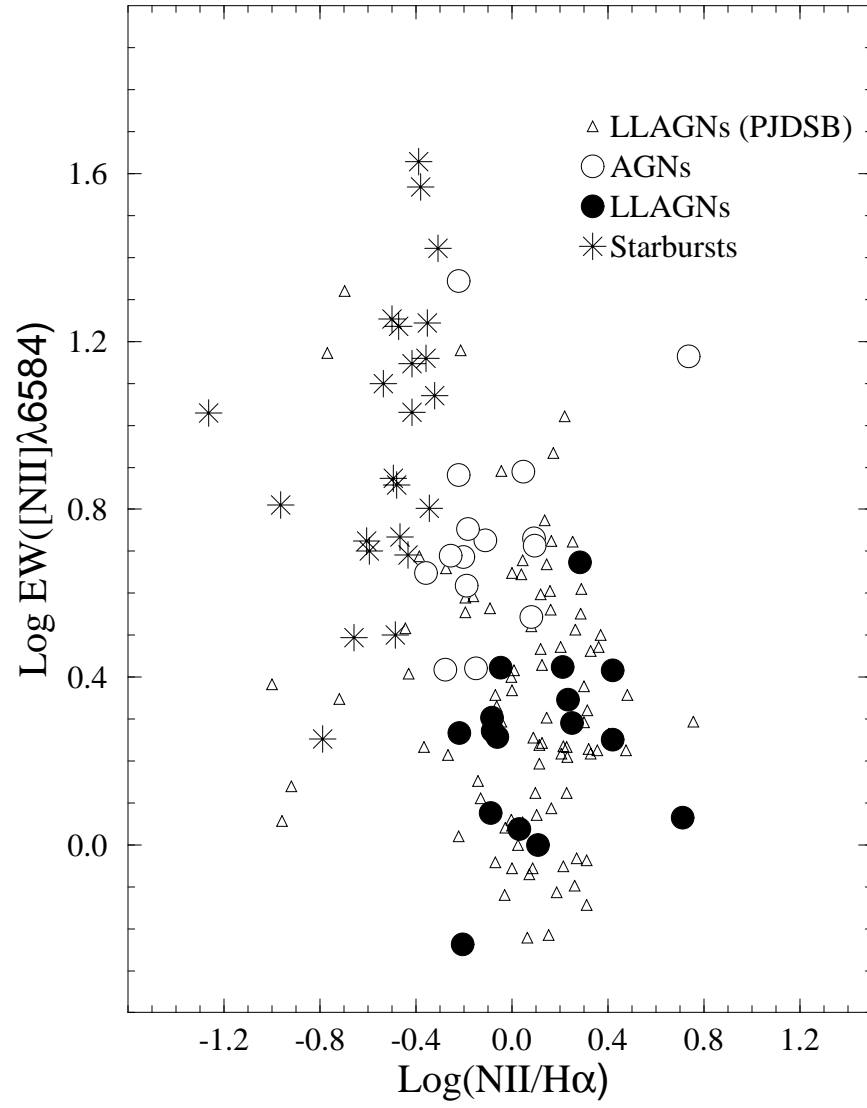


Fig. 5

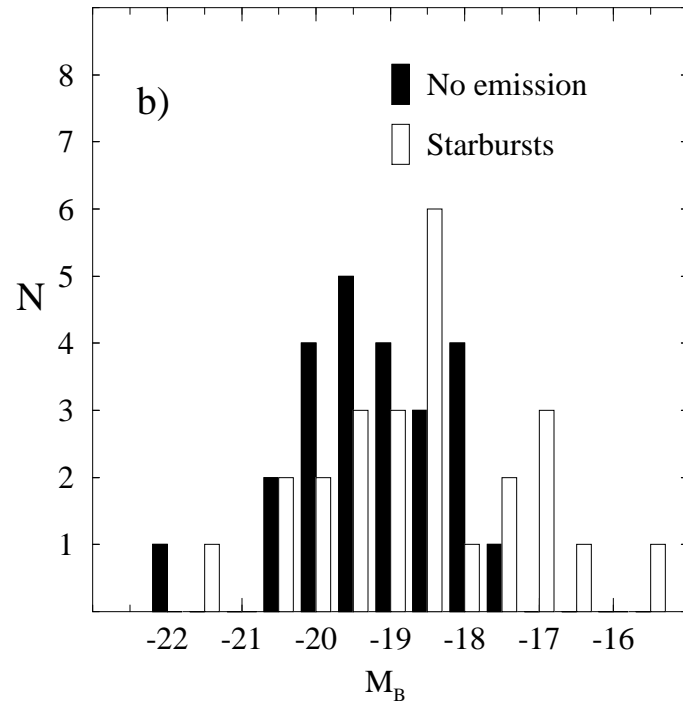
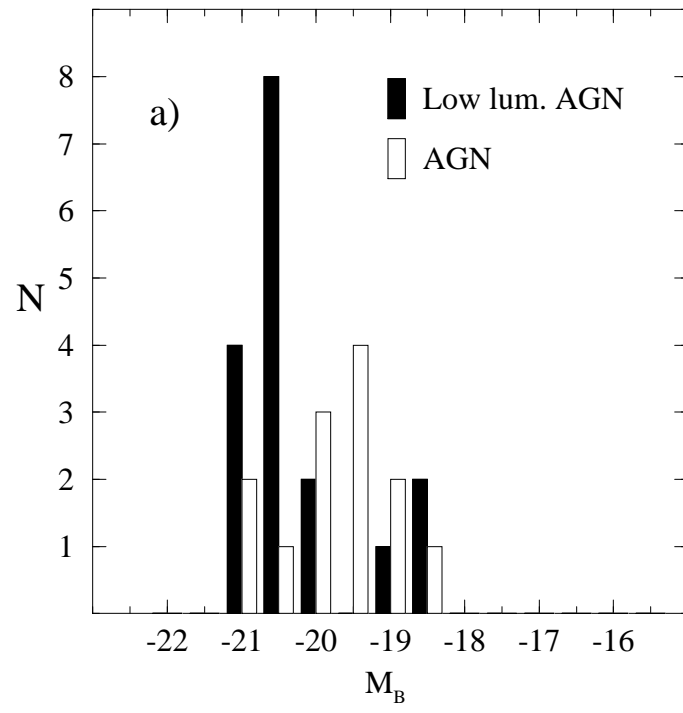


Fig. 6

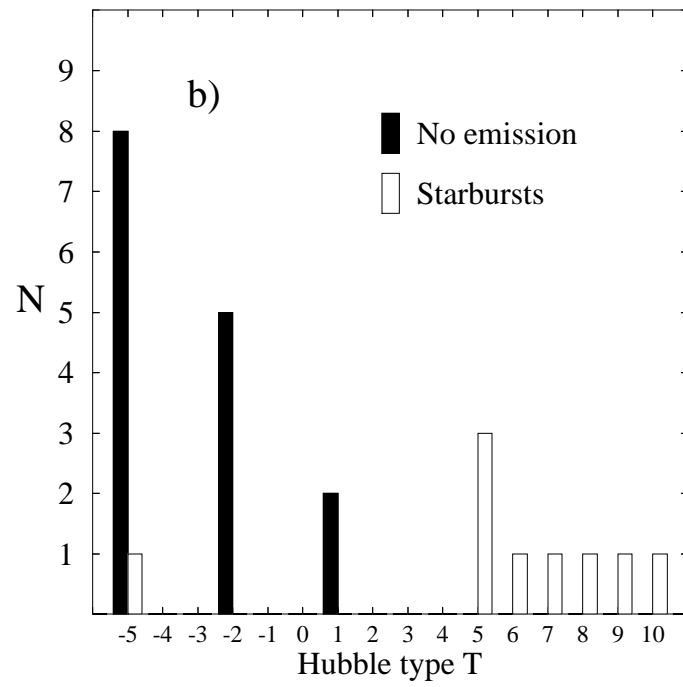
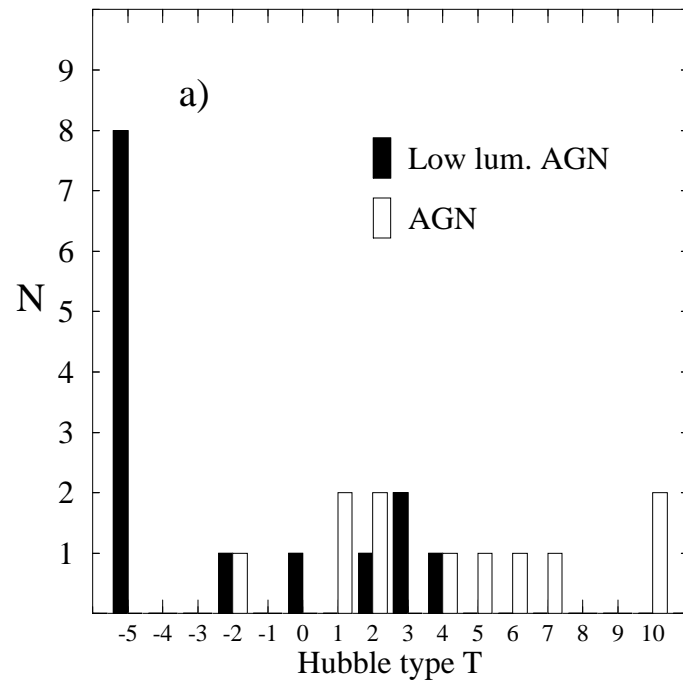


Fig. 7

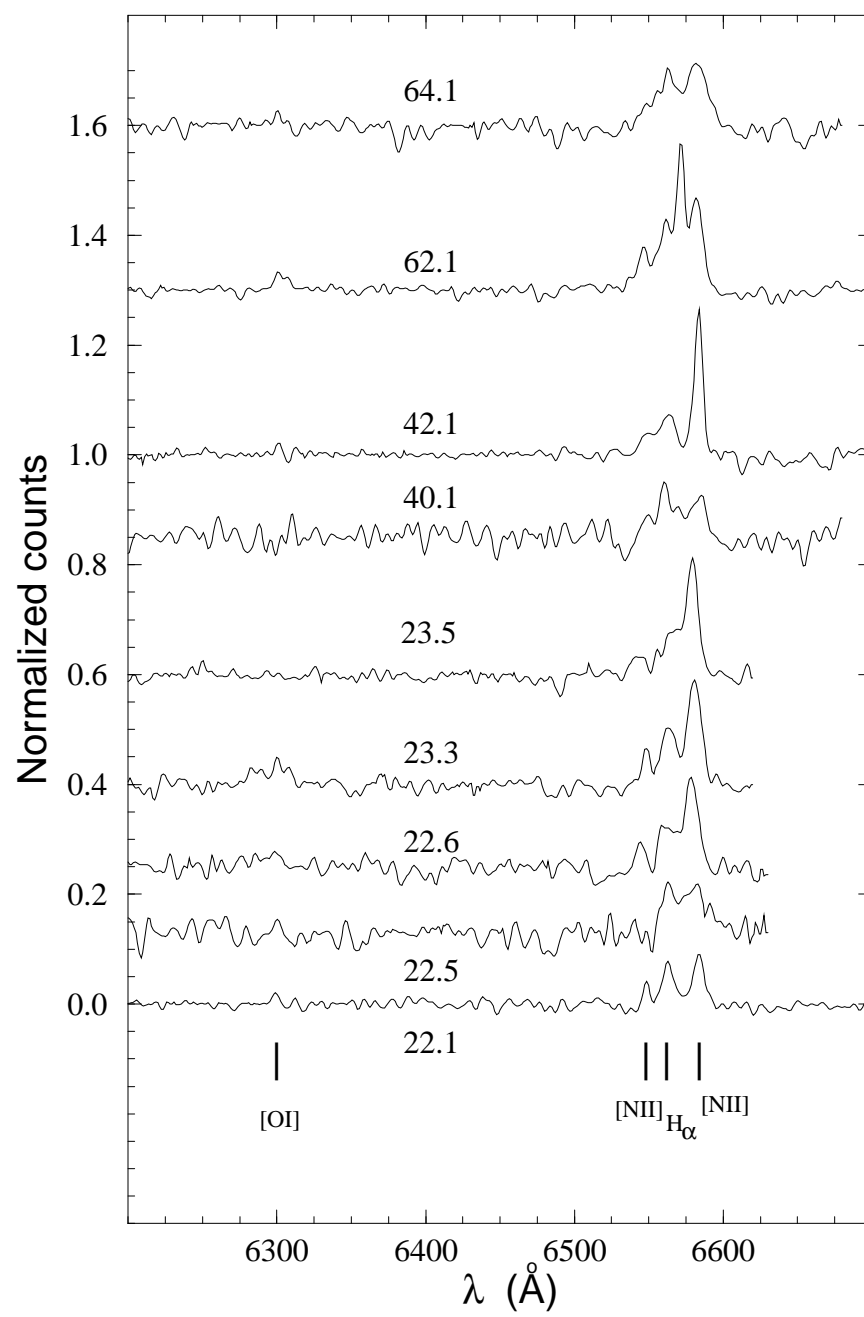


Fig. 2